Article

Mid-Infrared Plasmonic excitation in Indium Tin Oxide micro-hole arrays

Fausto D'apuzzo, Marco Esposito, Massimo Cuscunà, Alessandro Cannavale, Salvatore Gambino, Giuseppe e. Lio, Antonio De Luca, Giuseppe Gigli, and Stefano Lupi

ACS Photonics, **Just Accepted Manuscript** • DOI: 10.1021/acsphotonics.8b00214 • Publication Date (Web): 09 May 2018

Mid-Infrared Plasmonic excitation in Indium Tin Oxide micro-hole arrays

Fausto D'apuzzo[2], Marco Esposito*[3,4], Massimo Cuscunà[3], Alessandro Cannavale[5], Salvatore Gambino[3,4], Giuseppe E. Lio[6,7], Antonio De Luca[6,7], Giuseppe Gigli[3,4] and Stefano Lupi[1]

1. CNR-IOM and Department of Physics, University of Rome La Sapienza, P.le A. Moro 2, 00185, Rome, Italy

2. Advanced Light Source Division, Lawrence Berkeley National Laboratory, Berkeley, California 94720, USA

3. CNR NANOTEC- Istituto di Nanotecnologia, Polo di Nanotecnologia, c/o Campus Ecotekne, Via Monteroni, I-73100 Lecce, Italy

4. Dipartimento Mat-Fis Ennio De Giorgi, Università del Salento, I-73100 Lecce, Italy

5. Department of Civil Engineering and Architecture (DICAR), Politecnico di Bari, via Orabona 4, 70125 Bari (Italy)

6. CNR NANOTEC Institute of Nanotechnology, Rende 87036, Italy

7. University of Calabria, Department of Physics, Rende 87036, Italy

**Corresponding Author: marco.esposito@unisalento.it*

ABSTRACT

Transparent Conducting Oxides (TCOs) are emerging as possible alternative constituent materials to replace noble metals such as silver and gold for low-loss plasmonic applications in the Near-Infrared (NIR) and Mid-Infrared (MIR) regimes. In particular, TCO-based nanostructures are extensively investigated for biospectroscopy exploiting their surface enhanced infrared absorption (SEIRA). The latter enhances the absorption from vibrational and rotational modes of nearby bio-molecules making TCO nanostructures, a promising candidate for IR sensing applications. Nevertheless, in order to produce inexpensive devices for lab-on-chip diagnostics, it would be auspicable to achieve surface enhanced infrared absorption with very simple microstructures not requiring nano-size control.

In this work, we attempt to demonstrate SEIRA effect with the least challenging fabrication, μm-scale instead of nm-scale, by tailoring both device design and charge density of ITO film. We show that micro-periodic hole arrays in a ITO film are able to produce SEIRA via grating coupling. Such a study opens the way for innovative and disrupting biosensing devices.

Keywords: Transparent Conducting Oxides, Mid Infrared plasmon, Indium Tin Oxide, SEIRA, micro-hole arrays, dielectric.

The field of infrared plasmonics has seen a new dawn since the introduction of materials with lower carrier concentration such as grapheme, [1] highly-doped semiconductors and TCOs. [2,3] Because of a lower plasma frequency these materials allow plasmonic excitations to be resonant at TeraHertz (THz), MIR and NIR frequencies, furthermore they offer lower losses, [4,5] higher energy confinement [6] and dynamical control [7,8] with respect to the noble metals generally employed in plasmonic applications. Among these, TCOs offer some further advantages, namely: no interference from inter-band transitions (energy gap > 3 eV), inexpensive production (thanks to their role in the display market), mechanical stability and high doping solubility[3] to reach carrier concentration higher than those possible in semiconductors.

For these reasons TCOs, today largely used as transparent electrodes for touch-screens, solar-cells and thermal-screens, received renewed attention, in the research field, as active materials for tunable devices, such as electro-optical modulators, [8] ultra-fast all-optical modulator, [9] active substrates for Au-plasmonics [10,11] and finally as infrared plasmonic metals. [4] The first experimental work on Surface Plasmon Polaritons (SPPs) by reflectance measurements is on unpatterned Indium Tin Oxide (ITO)/dielectric interfaces [12,13], while only recently plasmonic nanostructures based on TCOs have been reported such as nanoparticles, [5,14,15] discs, [16] pillars, [17–21] dipole antennas, [22,23] split-ring resonators (SRR) [6] and Metal-Insulator-Metal stacks

(MIM), [24] with proof-of-principle demonstrations of their performance in metamaterials, [6] telecommunication [18] and Surface Enhanced Infrared Absorption (SEIRA) applications. [22,24,25] The SEIRA applications rely on the extreme energy confinement induced by SPPs and their consequent field enhancement. Nevertheless, the already published works on SEIRA [22,24] have demonstrated that TCO can hardly compete [6] with noble metals for plasmonic sensing applications, because of their weaker negative permittivity, while the poorer energy confinement in the MIR can be compensated by state-of-the-art nano-fabrication approaches providing nanostructured TCO, such as nano-sized gap-antennas. [26] As a consequence, TCO-based innovative devices for SEIRA applications [22,24] also rely on expensive nano-sized control of element dimensions for signal amplification, [23] but, in order to produce inexpensive devices for lab-on-chip diagnostics, fabrication constrains must be circumvented. Ideally, we would like TCOs SEIRA performances comparable to "gold-standard" devices, but with inexpensive micro-structures that don't require nano-size control.

In this work, we demonstrate SEIRA effect with the least challenging fabrication (μm-scales instead of tens of nm), by tailoring both device design and charge density of ITO films. We show that micro-periodic hole arrays in a ITO film are highly suitable for surface-enhanced infrared absorption.

By varying the grating pitch, it was possible to study the evolution of surface plasmon resonances (SPRs) in the spectral region of biological fingerprinting 600-1400 cm^{-1}, for a periodicity of the order of μm. The deposition parameters of ITO film are properly engineered to obtain a plasma frequency of about ω_p =5400 cm^{-1}, much below the commercial standard ITO (ω_p =12000 cm^{-1}), providing plasmonic effects in the biological fingerprint of the Mid-Infrared. The transmission data are supported by analytical models and numerical calculations. To our knowledge ITO hole arrays were previously investigated only theoretically for Near-Infrared gas sensing devices [27] and therefore at frequencies not suitable for SEIRA. Therefore, this is also the first experimental study of SPPs in TCO in the grating-coupling mechanism. Although we make use of ITO, we expect similar results for other TCOs, such as Indium-free AZO, GZO, FTO and FZO. [28]

RESULTS AND DISCUSSION

By controlling the deposition parameters in the ITO growth process, it was possible to control ITO optical and electrical properties, such as conductivity, transmittance and its carrier density. For this reason, several ITO films, with different sheet resistance from 16 up to 60 Ω/□ were grown on glass substrate in order to characterize the optical behaviour from the infrared to the ultraviolet spectral region (Figure S1). Furthermore, by increasing the sheet resistance up to 60 Ω/□ (see methods), the plasma frequency can be shifted by 6000 cm^{-1}, while leaving the transmittance in the visible range well above 80%. In order to achieve plasmonic effects in the biological fingerprint region of the Mid-Infrared (600-1400 cm^{-1}), the ITO film was sputtered on high-resistivity silicon substrate, which is transparent in this spectral region.

Four periodic hole arrays were fabricated on silicon substrate by electron beam lithography (EBL) using poly(methyl methacrylate) (PMMA) resist, obtaining patterns with periodicities p = 1, 2, 4, and 8 μm and diameters a = p/2. Then, a 60 nm thick ITO film was deposited by R.F. sputtering technique using deposition parameters optimized to produce film with 54 Ω/□ (see methods). Finally, the lift-off process was performed under sonication. Figures 1b-e show the SEM images of the patterned ITO micro-periodic hole-arrays with different geometrical features.

The ITO film was also deposited in unpatterned area as reference for optical measurements. Transmission measurements were performed on the 200x200 μm samples by means of a hyperion infrared microscope coupled to a Michelson interferometer. Transmittance is calculated as the ratio $T(\nu)=I_t(\nu)/I_0(\nu)$, where $I_t(\nu)$ is the light intensity transmitted by the sample and $I_0(\nu)$ is the one transmitted by the Si substrate.

The unpatterned ITO film exhibits a 40% absorption in the mid-infrared attributed to the free-carriers Drude component, conversely at higher frequency yields a transmittance above 85% (inset of Figure 1a). By fitting such optical transmission with the Tinkham formula [29] we have retrieved the microscopic parameters of the ITO film ω_p = 5400 cm^{-1}, Γ_D =250 cm^{-1} and the related complex permittivity by leveraging the Drude-Lorentz model (Figure S2). The real (ε′) and imaginary (ε″) parts were

also compared to literature data [30] related to a 150 nm thick commercial ITO (Geomatec Co. Ltd.) featured by a higher plasma frequency about 16700 cm^{-1}. As it can be seen, the magnitudes of ε′ and ε″ are smaller than those of commercial ITO because of the lower carrier density. In fact, our ITO film shows a higher resistivity of about 324 μΩ·cm, about three times larger than the one reported for Geomatec ITO. [30] It is worth noting that a very low damping rate value Γ_D of about 250 cm^{-1} as compared to 700 cm^{-1} of the commercial ITO, provides to further lower the ε″ magnitude in the Mid-Infrared range, providing an interesting low-loss material (Figure S2b). Such a low Γ_D value could be ascribed to the quite small layer thickness within which small grains are densely packed as reported in [30]. Such a permittivity indicates that properly tailored ITO is suitable as plasmonic material in the IR region.

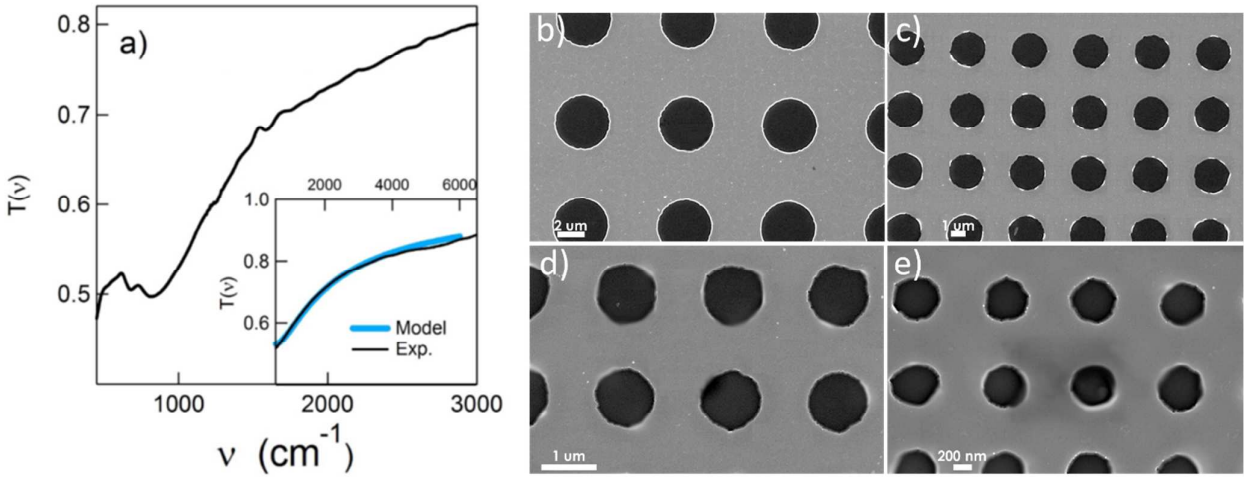

Figure 1. a) Infrared spectrum of patterned ITO (p = 1 μm) and unpatterned film deposited on Si substrate (inset). b)-e) SEM images of the patterned ITO with 8, 4, 2 and 1 μm lattice period, respectively.

In order to directly excite SPs by transmission measurements an extra wave vector is necessary and it can be provided by a periodic perturbation of the dielectric interface, a mechanism called grating coupling. The transmittance of the patterned ITO/Si is shown in Figure 1a, for p=1 μm, where the Drude slope is clearly visible, but modified between 800 and 1500 cm^{-1} by a plasmonic mode. In noble metals, [31] a similar structure would exhibit an extraodinary optical transmission (EOT) peak [32] with a characteristic asymmetric Fano-profile [33] over a slow-varying background, conversely, ITO is not completely opaque at these frequencies, hence the plasmonic mode appears as a modulation of the Drude plasma edge.

The optical response of micro-periodic hole arrays strongly evolves by tuning the grating pitch from 1 to 8 μm as shown in Figure 2, where the differential extinction $1-T(\nu)/T_0(\nu)$ is plotted to enhance the plasmonic modulation with respect to the underlying Drude component ($T_0(\nu)$). Here the plasmonic mode appears as a broad absorption peak in the p = 1 μm sample, and also we can clearly see that the plasmonic peak shifts to lower energies for increasing p, as expected from plasmonic thumb-rules. In fact, the p = 2 μm shows an even stronger peak at slightly lower frequencies, between 600 and 1400 cm^{-1}, while for the samples with p = 4 and 8 μm, the peak intensity is strongly decreased, and appears as a small kink.

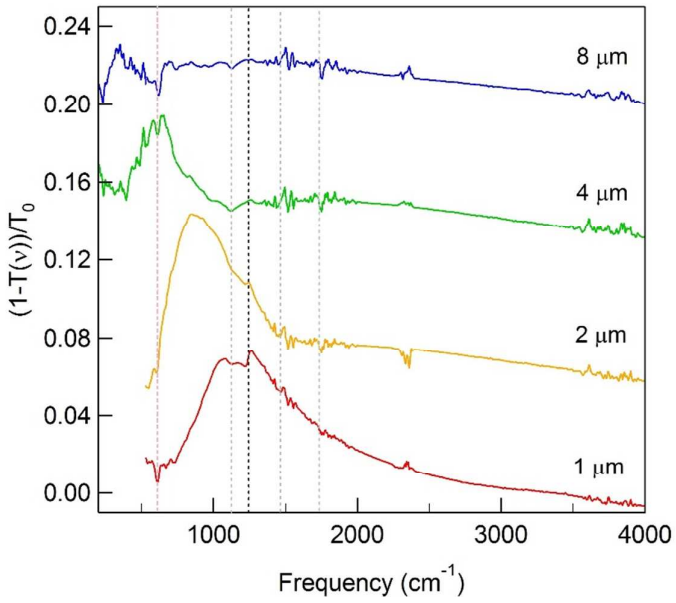

Figure 2. Differential extinction spectra for ITO/Si grating with periodicity from 1 to 8 μm. The evolution of the mode shows a strong shift of the peak frequency for p increasing. Pink dashed line indicates the phonon mode, while black dashed lines highlight the PMMA vibrational modes.

A detailed study of the above mentioned resonances is shown in Figure 3 reporting the frequency-wavevector (ν,q) dispersion, where the experimental frequency (red solid squares) is plotted as a function of the inverse periodicity $p^{-1}=q/2\pi$. The larger gratings with p^{-1} = 1250 and 2500 cm^{-1}, follow a linear dispersion superimposed to the light line for the ITO/Si interface (shaded area) which confirms their correct identification. It is worth noting that plasmons at the ITO/Air interface, expected at higher frequency (above 3000 cm^{-1}), are not observed (see Figure 2) because ITO film becomes more and more transparent. These modes show the same ν_p,q values as those of free electromagnetic waves in silicon and therefore have a photonic-like character. [34] Such modes can be interpreted as a diffraction order grazing the sample surface and are observed in any metal grating independently of their plasma frequency, as experimentally reported for Au/Si interface (gold solid squares). [35] These modes are known as spoof plasmons and they are really weak because a p/2= 4 micron hole at λ = 30 μm is sub-wavelength and its transmission coefficient is intrinsically low.

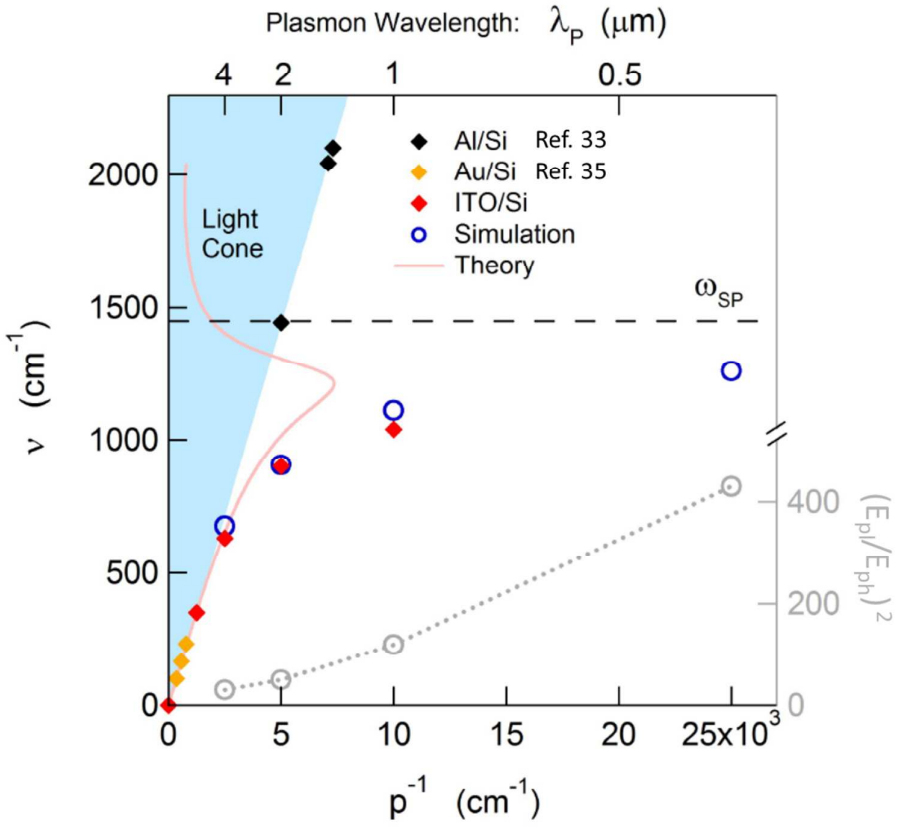

Figure 3. Dispersion diagram of the ITO/Si hole arrays (red solid squares). Modes evolution from photonic-like regime along the light-line (shaded area) to Surface Plasmon frequency ω_{SP} limit (dashed line) also reported the theoretical SP dispersion curve from standard Surface Plasmon [36] (pink solid line). Comparison with similar structure made of noble Metal/dielectric interfaces (orange and black symbols) is reported from literature. Numerically calculated field-enhancement at the resonant frequencies of the hole arrays with periodicity from 1 to 8 μm between the maximum plasmonic field E_{pl} and that one of the incoming wave E_{ph} (right axis).

When the resonance mode approaches the surface plasmon (SP) frequency, (dashed horizontal line):

$$\omega_{SP} = \frac{\omega_p}{\sqrt{1+\epsilon_{Si}}} = 1490\ cm^{-1}$$

where ε_{si} = 11.9 is the dielectric constant of silicon in the infrared range, the dispersion bends away from the light line entering into the plasmonic regime. At this higher q, the energy confinement is stronger and the plasmon frequency saturates towards the asymptotic ω_{SP} value. The comparison with hole arrays of same periodicity (p^{-1}=5000 cm^{-1}), but made of an Al/Si interface [33], shows that noble metals strictly follow the photonic-like dispersion from the far-infrared through the whole Mid-Infrared spectrum requiring higher q, and thus more challenging nano-fabrication, in order to enter into the plasmonic-regime. Hence, there is no intrinsic plasmonic confinement, highlighting the significant advantages of using low plasma frequency metals such as ITO.

Our experimental results are also consistent with both Far-Infrared spoof plasmons in Au/Si interfaces [35] (gold solid squares), as well as with the analytical model of standard Surface Plasmon theory (pink solid line in Figure 3) for 3D metals. [36]

The maximum value of p^{-1} at around 10000 cm^{-1} represents the last SP that can propagate, beyond which the mode becomes over damped and can only exist as a localized surface plasmon. The reported dispersion is further confirmed by

electromagnetic simulations of the ITO hole array performed using the CST Microwave Studio commercial software, using the ITO dielectric function reported in Figure S2. The simulations yield resonance frequencies (blue open circles) in very good agreement with experimental data, and show how the field enhancement is localized at the edge of the holes corresponding to the triple interface ITO/Si/Air (see Figure S3); this hot spot volume is therefore accessible for SEIRA sensing applications. Furthermore the simulation offers the possibility to extrapolate beyond experimental reach, up to a period of p=400 nm, approaching the asymptotic SP frequency $\omega_{sp} = 1490$ cm^{-1}.

A parameter that is not easily measured experimentally is the field-enhancement (FE), defined as the maximum plasmonic electric field E_{max} and that of incident light E_0 away from the structure, $FE=E_{max}/E_0$. Electromagnetic simulation yields values of FE (right axis in Figure 3) that range from around ten, for the photonic regime, to few hundreds for the full plasmonic gratings, as a consequence of the k_p/k_0 squeezing effect with k_p defined as:

$$k_p = Re\left[\frac{\nu}{c}\sqrt{\frac{\epsilon_m \epsilon_{si}}{\varepsilon_{m+\epsilon_{si}}}}\right]$$

where $\varepsilon_m(\nu)$ is the complex dielectric function of the ITO, with its parameters as retrieved from measurements on the unpatterned film.

A route to experimentally observe the microscopic enhancement of the plasmonic near-field is to use the device as a SEIRA sensor by depositing a small quantity of target in the plasmonic hot-spots, and look for enhancement of the target vibrational fingerprint.

As a serendipitous result of the fabrication process, small residues of PMMA are present around a portion of the aperture edges at the ITO/Air and ITO/Si interfaces due to non-optimal PMMA development and lift-off steps as better described in the supplementary information (Figure S4). Vibrational modes of PMMA are C-O-C (1140 cm^{-1}), C-O (1250 cm^{-1}), C-H (1450 cm^{-1}) and C=O (1720 cm^{-1}) stretching modes (black dashed lines in Figure 2). While the C-H and C=O are in the noisy range of atmospheric absorption, and the C-O-C bond absorption is strongly reduced due to the effect of electron beam illumination (which actually breaks the polymer main bonds), the C-O at 1250 cm^{-1} is clearly visible as a modulation of the plasmonic peak. Another feature at 650 cm^{-1} is visible in all spectra, and may correspond to some of the phonons of the silicon substrate (pink dashed lines in Figure 2).

The absorption at 1250 cm^{-1} is prominent in the plasmonic regime samples (p = 2 and 1 μm) while is almost absent in the photonic-like spectra (p = 8 and 4 μm). That portion of the spectrum, compensated for their respective baseline is reported in Figure 4a, where the gradual plasmonic enhancement is evident. Because the residual PMMA is randomly distributed, as better described in supplementary information (Figure S4), hence, its amount over the samples is very low and not very different from each other. In the photonic-regime no enhancement is expected and any signal is under the noise level. Instead, as the mode acquires a more plasmonic character the absorption increases significantly, now with a S/N ~ 10, and becomes asymmetric, signature of a Fano-like plasmon-phonon interaction. This is one of the first demonstration of the capabilities of TCOs, such as ITO, to effectively produce SEIRA via grating coupling in micro-structures.

This experiment provides an indirect measurement of the near-field plasmonic enhancement, in fact the peak-to-peak intensity of the 1250 cm^{-1} line is increased by a factor 10 above noise. The enhanced Infrared signal can be compared with the simulated near-field enhancement reported in Figure 4b again as a function of the inverse lattice period (gray symbols). The S/N ratio from Figure 4a is reported (red symbols) in comparison with the simulation by matching the scale. The slope of the experimental data is in very good agreement with the numerical results, especially taking into account that the noise level is responsible for an overestimation of the two lowest data points related to p = 8 and 4 μm. By numerical verification, of the

experimental data, we can confidently assert that a SEIRA signal could reach a factor 100 enhancement with respect to the non-plasmonic regime with even smaller arrays.

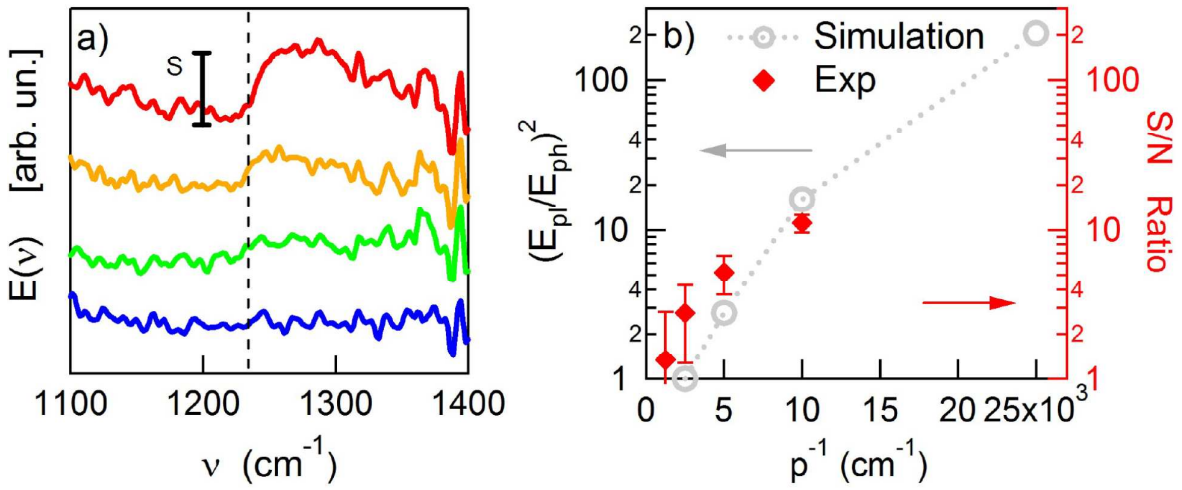

Figure 4. a) SEIRA enhancement of the vibrational line of PMMA at 1250 cm^{-1} in the extinction spectra of the ITO/Si gratings subtracted of their baselines. b) Numerical calculation of field enhancement due to plasmonic effects (gray circles) and experimental data (red solid squares) of the Signal/Noise (S/N) ratio at the 1250 cm^{-1} absorption line.

CONCLUSIONS

In conclusion, we report ITO sensing performances at MIR frequencies by exploiting its plasmonic properties. Our results show that ITO sensing performances go beyond that of noble metals. In particular, the plasmonic effects can be obtained by using microstructures of 2 μm periodicity without the need of nano-size control of the structural antenna design. This result is possible because of the intrinsic energy confinement provided by this suitable infrared material. Therefore, we can expect TCOs plasmonic applications to leverage on this advantage to produce cheap and performing SEIRA sensors for biomedical applications.

METHODS

Two-dimensional hole arrays were fabricated by electron beam lithography on a silicon substrate. After cleaning the substrate in acetone and 2-propanol, a 500 nm PMMA layer was spin coated on the substrate at 2500 rpm and soft-baked at 180 °C for 3 min. Subsequently, in order to obtain arrays of holes, a negative pattern was designed and written by a Raith 150 system at 22 pA beam current and 30 keV. After the exposure, a MIBK:IPA solution in a 1:3 ratio for 3 min and rinsed in 2-propanol for 1 min was used to develop the resist.

ITO ($Sn:In_2O_3$) films with a thickness of about 60 nm were deposited by high vacuum RF sputtering on the pre-patterned PMMA-glass substrate. The base pressure inside the vacuum chamber was initially 10^{-7} mbar and then a pure dry Argon flux (10 sccm) was used without adding oxygen (non-reactive). The pressure then dropped to 10^{-4} mbar and was kept constant throughout the whole deposition process. The RF power was 75 W, which led to a deposition rate of ~ 0.4 Å/s. The substrate temperature was kept at RT during the whole process. Finally, a liftoff process, under sonication, was performed in mr-Rem 500 remover solution (Microresist Technology) for 20 minutes and rinsed in 2-propanol.

Material deposition parameters were optimized at RT on glass substrate in order to simultaneously: tune the plasma frequency in the desired range and to obtain a material thickness skilled to enable efficient lift-off process. In this case, the resistivity and the sheet resistance are determined as a function of the material thickness.

A complete electrical characterization of ITO films on glass were performed in air and at RT conditions using an Ecopia 3100 system in the Van der Paw configuration where gold tips were placed on the four corners of squared samples. High mobility value of 41 cm^2/Vs was observed together with a sheet resistance of 54 Ω/□.

Transmission measurements were performed on the 200x200 μm^2 samples by means of a Hyperion FTIR microscope (Bruker) coupled to a Michelson interferometer.

Numerical simulations were performed by CST Microwave Studio.

Conflicts of interest

There are no conflicts to declare

AWKNOWLEDGEMENTS

This work was partly sponsored by the national projects "Molecular Nanotechnologies for Health and Environment" (MAAT, PON02_00563_3316357 and CUPB31C12001230005).

REFERENCES

(1) Low, T.; Avouris, P. Graphene Plasmonics for Terahertz to Mid-Infrared Applications. *ACS Nano* **2014**, *8* (2), 1086–1101.
(2) Boltasseva, A.; Atwater, H. A. Low-Loss Plasmonic Metamaterials. *Science* **2011**, *331* (6015), 290–291.
(3) Naik Gururaj V.; Shalaev Vladimir M.; Boltasseva Alexandra. Alternative Plasmonic Materials: Beyond Gold and Silver. *Adv. Mater.* **2013**, *25* (24), 3264–3294.
(4) West P.R.; Ishii S.; Naik G.V.; Emani N.K.; Shalaev V.M.; Boltasseva A. Searching for Better Plasmonic Materials. *Laser Photonics Rev.* **2010**, *4* (6), 795–808.
(5) Johns, R. W.; Bechtel, H. A.; Runnerstrom, E. L.; Agrawal, A.; Lounis, S. D.; Milliron, D. J. Direct Observation of Narrow Mid-Infrared Plasmon Linewidths of Single Metal Oxide Nanocrystals. *Nat. Commun.* **2016**, *7*, 11583.
(6) Gregory, S. A.; Wang, Y.; de Groot, C. H.; Muskens, O. L. Extreme Subwavelength Metal Oxide Direct and Complementary Metamaterials. *ACS Photonics* **2015**, *2* (5), 606–614.
(7) Rodrigo, D.; Limaj, O.; Janner, D.; Etezadi, D.; Abajo, F. J. G. de; Pruneri, V.; Altug, H. Mid-Infrared Plasmonic Biosensing with Graphene. *Science* **2015**, *349* (6244), 165–168.
(8) Melikyan, A.; Lindenmann, N.; Walheim, S.; Leufke, P. M.; Ulrich, S.; Ye, J.; Vincze, P.; Hahn, H.; Schimmel, T.; Koos, C.; et al. Surface Plasmon Polariton Absorption Modulator. *Opt. Express* **2011**, *19* (9), 8855–8869.
(9) Kinsey, N.; DeVault, C.; Kim, J.; Ferrera, M.; Shalaev, V. M.; Boltasseva, A. Epsilon-near-Zero Al-Doped ZnO for Ultrafast Switching at Telecom Wavelengths. *Optica* **2015**, *2* (7), 616–622.
(10) Abb, M.; Albella, P.; Aizpurua, J.; Muskens, O. L. All-Optical Control of a Single Plasmonic Nanoantenna–ITO Hybrid. *Nano Lett.* **2011**, *11* (6), 2457–2463.
(11) Zhu, Y.; Hu, X.; Fu, Y.; Yang, H.; Gong, Q. Ultralow-Power and Ultrafast All-Optical Tunable Plasmon-Induced Transparency in Metamaterials at Optical Communication Range. *Sci. Rep.* **2013**, *3*, 2338.
(12) Rhodes, C.; Franzen, S.; Maria, J.-P.; Losego, M.; Leonard, D. N.; Laughlin, B.; Duscher, G.; Weibel, S. Surface Plasmon Resonance in Conducting Metal Oxides. *J. Appl. Phys.* **2006**, *100* (5), 054905.
(13) Franzen, S. Surface Plasmon Polaritons and Screened Plasma Absorption in Indium Tin Oxide Compared to Silver and Gold. *J. Phys. Chem. C* **2008**, *112* (15), 6027–6032.
(14) Kanehara, M.; Koike, H.; Yoshinaga, T.; Teranishi, T. Indium Tin Oxide Nanoparticles with Compositionally Tunable Surface Plasmon Resonance Frequencies in the Near-IR Region. *J. Am. Chem. Soc.* **2009**, *131* (49), 17736–17737.
(15) Garcia, G.; Buonsanti, R.; Runnerstrom, E. L.; Mendelsberg, R. J.; Llordes, A.; Anders, A.; Richardson, T. J.; Milliron, D. J. Dynamically Modulating the Surface Plasmon Resonance of Doped Semiconductor Nanocrystals. *Nano Lett.* **2011**, *11* (10), 4415–4420.
(16) Kim, J.; Naik, G. V.; Emani, N. K.; Guler, U.; Boltasseva, A. Plasmonic Resonances in Nanostructured Transparent Conducting Oxide Films. *IEEE J. Sel. Top. Quantum Electron.* **2013**, *19* (3), 4601907–4601907.
(17) Li, S. Q.; Guo, P.; Zhang, L.; Zhou, W.; Odom, T. W.; Seideman, T.; Ketterson, J. B.; Chang, R. P. H. Infrared Plasmonics with Indium–Tin-Oxide Nanorod Arrays. *ACS Nano* **2011**, *5* (11), 9161–9170.
(18) Li, S.-Q.; Guo, P.; Buchholz, D. B.; Zhou, W.; Hua, Y.; Odom, T. W.; Ketterson, J. B.; Ocola, L. E.; Sakoda, K.; Chang, R. P. H. Plasmonic–Photonic Mode Coupling in Indium-Tin-Oxide Nanorod Arrays. *ACS Photonics* **2014**, *1* (3), 163–172.
(19) Li, S.-Q.; Sakoda, K.; Ketterson, J. B.; Chang, R. P. H. Broadband Resonances in Indium-Tin-Oxide Nanorod Arrays. *Appl. Phys. Lett.* **2015**, *107* (3), 031104.

(20) Khosroabadi Akram A.; Gangopadhyay Palash; Duong Binh; Thomas Jayan; Sigdel Ajaya K.; Berry Joseph J.; Gennett Thomas; Peyghambarian N.; Norwood Robert A. Fabrication, Electrical and Optical Properties of Silver, Indium Tin Oxide (ITO), and Indium Zinc Oxide (IZO) Nanostructure Arrays. *Phys. Status Solidi A* **2013**, *210* (5), 831–838.

(21) Riley Conor T.; Kieu Tien A.; Smalley Joseph S. T.; Pan Si Hui Athena; Kim Sung Joo; Post Kirk W.; Kargar Alireza; Basov Dimitri N.; Pan Xiaoqing; Fainman Yeshaiahu; et al. Plasmonic Tuning of Aluminum Doped Zinc Oxide Nanostructures by Atomic Layer Deposition. *Phys. Status Solidi RRL – Rapid Res. Lett.* **2014**, *8* (11), 948–952.

(22) Abb, M.; Wang, Y.; Papasimakis, N.; de Groot, C. H.; Muskens, O. L. Surface-Enhanced Infrared Spectroscopy Using Metal Oxide Plasmonic Antenna Arrays. *Nano Lett.* **2014**, *14* (1), 346–352.

(23) Black, L.-J.; Wang, Y.; Abb, M.; Boden, S. A.; Groot, C. H. de; Arbouet, A.; Muskens, O. L. New Plasmonic Materials and Fabrication Tools for near- and Mid-Infrared Sensing and Spectroscopy. In *Chemical, Biological, Radiological, Nuclear, and Explosives (CBRNE) Sensing XVI*; International Society for Optics and Photonics, 2015; Vol. 9455, p 94550K.

(24) Kim, J.; Dutta, A.; Memarzadeh, B.; Kildishev, A. V.; Mosallaei, H.; Boltasseva, A. Zinc Oxide Based Plasmonic Multilayer Resonator: Localized and Gap Surface Plasmon in the Infrared. *ACS Photonics* **2015**, *2* (8), 1224–1230.

(25) Chen, K.; Guo, P.; Dao, T. D.; Li, S.-Q.; Ishiii, S.; Nagao, T.; Chang, R. P. H. Protein-Functionalized Indium-Tin Oxide Nanoantenna Arrays for Selective Infrared Biosensing. *Adv. Opt. Mater.* **2017**, *5* (17), 1700091.

(26) Huck, C.; Neubrech, F.; Vogt, J.; Toma, A.; Gerbert, D.; Katzmann, J.; Härtling, T.; Pucci, A. Surface-Enhanced Infrared Spectroscopy Using Nanometer-Sized Gaps. *ACS Nano* **2014**, *8* (5), 4908–4914.

(27) Tanasković, D.; Jakšić, Z. Enhancing Performance of Nanohole-Based Plasmonic Sensors by Transparent Conductive Oxides. In *2012 28th International Conference on Microelectronics Proceedings*; 2012; pp 199–202.

(28) Calzolari, A.; Ruini, A.; Catellani, A. Transparent Conductive Oxides as Near-IR Plasmonic Materials: The Case of Al-Doped ZnO Derivatives. *ACS Photonics* **2014**, *1* (8), 703–709.

(29) Glover, R. E.; Tinkham, M. Conductivity of Superconducting Films for Photon Energies between 0.3 and $40k{T}_{c}$. *Phys. Rev.* **1957**, *108* (2), 243–256.

(30) Tamanai Akemi; Dao Thang Duy; Sendner Michael; Nagao Tadaaki; Pucci Annemarie. Mid□infrared Optical and Electrical Properties of Indium Tin Oxide Films. *Phys. Status Solidi A* **2016**, *214* (3), 1600467.

(31) Scuderi, M.; Esposito, M.; Todisco, F.; Simeone, D.; Tarantini, I.; De Marco, L.; De Giorgi, M.; Nicotra, G.; Carbone, L.; Sanvitto, D.; et al. Nanoscale Study of the Tarnishing Process in Electron Beam Lithography-Fabricated Silver Nanoparticles for Plasmonic Applications. *J. Phys. Chem. C* **2016**, *120* (42), 24314–24323.

(32) Ghaemi, H. F.; Thio, T.; Grupp, D. E.; Ebbesen, T. W.; Lezec, H. J. Surface Plasmons Enhance Optical Transmission through Subwavelength Holes. *Phys. Rev. B* **1998**, *58* (11), 6779–6782.

(33) Limaj, O.; D'Apuzzo, F.; Di Gaspare, A.; Giliberti, V.; Domenici, F.; Sennato, S.; Bordi, F.; Lupi, S.; Ortolani, M. Mid-Infrared Surface Plasmon Polariton Sensors Resonant with the Vibrational Modes of Phospholipid Layers. *J. Phys. Chem. C* **2013**, *117* (37), 19119–19126.

(34) Todisco, F.; Esposito, M.; Panaro, S.; De Giorgi, M.; Dominici, L.; Ballarini, D.; Fernández-Domínguez, A. I.; Tasco, V.; Cuscunà, M.; Passaseo, A.; et al. Toward Cavity Quantum Electrodynamics with Hybrid Photon Gap-Plasmon States. *ACS Nano* **2016**, *10* (12), 11360–11368.

(35) D'Apuzzo, F.; Candeloro, P.; Domenici, F.; Autore, M.; Pietro, P. D.; Perucchi, A.; Roy, P.; Sennato, S.; Bordi, F.; Fabrizio, E. M. D.; et al. Resonating Terahertz Response of Periodic Arrays of Subwavelength Apertures. *Plasmonics* **2015**, *10* (1), 45–50.

(36) Maier, S. A. *Plasmonics: Fundamentals and Applications*; Springer US, 2007.

TOC

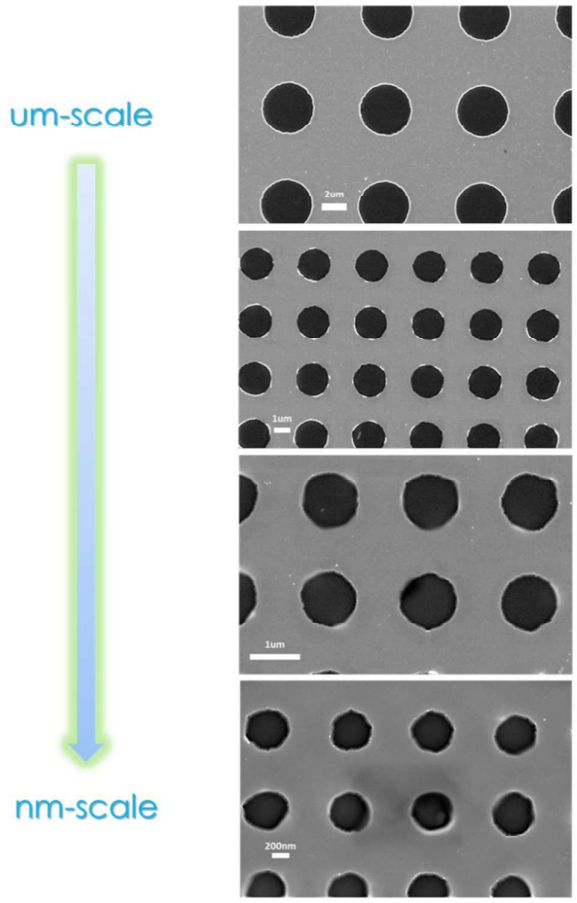
um-scale
nm-scale
2um
1um
1um
200nm

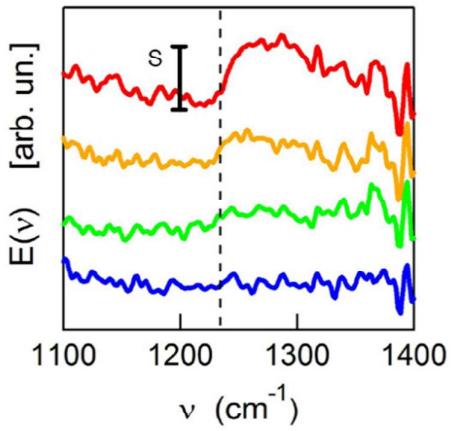
S
E(ν) [arb. un.]
1100
1200
1300
1400
ν (cm-1)

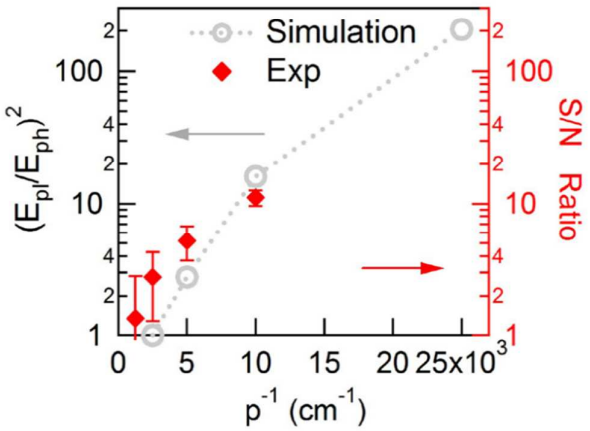
Simulation
Exp
(Epl/Eph)2
S/N Ratio
p-1 (cm-1)
0
5
10
15
20
25x10^3